NLRP3 inflammasome expression affects immune cell infiltration and clinical prognosis in *Helicobacter pylori* infection-associated gastric cancer

CHUANDAN WAN[1*], YEQIONG XU[1*], YANPING ZHU[1], XUEXIAN CAO[2], PING WANG[3] and YULAN GU[2]

[1]Central Laboratory, Changshu Medical Examination Institute, Changshu, Jiangsu 215500, P.R. China; [2]Department of Oncology and Radiotherapy, Affiliated Changshu Hospital of Nantong University, Changshu, Jiangsu 215500, P.R. China; [3]School of Basic Medical Sciences, Wannan Medical College, Wuhu, Anhui 241002, P.R. China

Received October 10, 2024; Accepted February 26, 2025

DOI: 10.3892/mmr.2025.13550

Abstract. High *Helicobacter pylori* infection rates contribute to high gastric cancer (GC) incidence. While *H. pylori* infection is associated with GC development its mechanisms are still being studied. The aim of the present study was to examine the differences between *H. pylori* infection-induced GC and non-infected tissues, and to investigate the correlation between nucleotide-binding oligomerization domain, leucine rich repeat and pyrin domain containing 3 (NLRP3) inflammasome expression and immune cell infiltration in GC, thus providing a theoretical basis for clinical prognosis and immunotherapy. High-throughput RNA-sequencing expression data from The Cancer Genome Atlas (TCGA) were analyzed. Additionally, TIMER2.0 and Kaplan-Meier Plotter were used to analyze the differential expression of NLRP3 mRNA in various tumors, the effect of *H. pylori* infection on gene expression, and the association between NLRP3 and clinical prognosis among patients with GC. Immunohistochemistry (IHC) was used to assess the effects of NLRP3 protein expression on immune cell infiltration in clinical tissues with or without *H. pylori* infection. R software was used for data visualization and statistical analysis. TCGA data revealed that the expression levels of NLRP3 in GC tissues were increased compared with those in normal tissues (P<0.05), which was further validated in clinical samples. Furthermore, NLRP3 mRNA expression was significantly elevated in clinical GC tissues infected with *H. pylori*. Notably higher relative levels of NLRP3 mRNA were observed in tumor tissues with a tumor size ≥5 cm, lymph node metastasis, Tumor-Node-Metastasis stage III + IV or poor differentiation compared with the respective controls (P<0.05). IHC confirmed a significant increase in NLRP3 expression within *H. pylori*-infected GC tissues compared with that in non-infected tissues. In GC immune infiltration, NLRP3 expression was revealed to be associated with natural killer cell, whereas it was negatively correlated with regulatory T cells and $CD8^+$ T cells. These findings indicated that NLRP3 may promote the polarization of tumor-associated macrophages towards the M2 phenotype. High NLRP3 expression also promoted the infiltration of $CD3^+$ and $CD206^+$ cells, which significantly affected the survival rate of patients with GC. The immune infiltration of regulatory T lymphocytes was associated with better survival benefits for patients with GC; however, M2 macrophage infiltration was not conducive to the survival of patients with GC. Furthermore, survival analysis showed that high expression of NLRP3 was associated with a poorer 5-year overall survival, progression-free survival and post-progression survival rates. In conclusion, elevated NLRP3 expression, which may be induced by *H. pylori* infection, could promote immune cell infiltration potentially by regulating cancer cell proliferation and migration, ultimately leading to an unfavorable prognosis and a notable reduction in the 5-year survival rate.

Correspondence to: Professor Yulan Gu, Department of Oncology and Radiotherapy, Affiliated Changshu Hospital of Nantong University, 18 Changshu Taishan Road, Changshu, Jiangsu 215500, P.R. China
E-mail: guyulan@263.net

Professor Ping Wang, School of Basic Medical Sciences, Wannan Medical College, 22 Wenchang West Road, Wuhu, Anhui 241002, P.R. China
E-mail: wangpingwnmc@wnmc.edu.cn

*Contributed equally

Key words: NLRP3 inflammasome, immune cell infiltration, gastric cancer, *Helicobacter pylori*, immunotherapy, prognosis

Introduction

The occurrence and development of gastric cancer (GC) are predominantly associated with *Helicobacter pylori* infection (1-3). Recent advances in medical detection technologies, along with innovative approaches to GC treatment, have resulted in a 5-year survival rate approaching 95% for individuals diagnosed with early-stage cancer; however, the majority of patients with GC are diagnosed with advanced stage cancer, resulting in an unfavorable prognosis and a low 5-year survival rate (1). The primary challenge hindering timely diagnoses

lies in the absence of screening tools possessing suitable sensitivity, specificity and practicality (1). The management of advanced GC primarily encompasses targeted drug therapy, immunotherapy and neoadjuvant chemotherapy (2). Unlike directly targeting the tumor itself, the objective of immunotherapy is to overcome immunosuppression induced by the tumor microenvironment to allow the innate immune system to target and eliminate cancer cells (2). Stromal cells, immune cells, vascular endothelium and intravascular blood cells are all present in tumor tissues, along with tumor cells. Immune cells contribute to the tumor microenvironment and perform a crucial function, known as tumor immune infiltration (3).

The presence of immune cells infiltrating into the tumor microenvironment is associated with the proliferation, invasion and spread of tumor cells. The various forms of immune cells that infiltrate into tumor tissues have a strong association with tumor classification and have a substantial impact on the response to immunotherapy, as well as the survival and prognosis of patients (4). The immune cells that infiltrate the tumor microenvironment not only attack cancer cells to prevent their growth, but also filter out which cancer cells are capable of surviving in the environment, potentially facilitating the progression of the tumor. Tumor immunotherapy is a crucial area of current research in cancer therapeutics. Distinguishing the specific type of immune infiltration in tumors can potentially indicate the efficacy of tumor immunotherapy (5). Immunotherapy based on immune checkpoint inhibitors has resulted in a new era of tumor treatment; therefore, identifying biomarkers to predict which patients are likely to benefit from tumor immunotherapy is important (6,7).

Nucleotide-binding oligomerization domain, leucine rich repeat and pyrin domain containing (NLRP) proteins form inflammasomes, which serve a crucial role in innate immunity and inflammatory responses (8). As an inflammatory response sensor signaling protein, NLRP mediates the activation of proteases to induce cytokine maturation and contributes to pyroptosis (9). Different NLRP members are expressed in various organs and tissues, participating in the occurrence and progression of different types of cancer by regulating innate and adaptive immune responses, cell death and proliferation (10). Among the inflammasome family members, NLRP3 is the most important member and is involved in a range of regulatory mechanisms (9). Certain cytokines, such as IL-1β precursors, require caspase activation by NLRP inflammasomes in the cytoplasm, particularly NLRP3 (11), which activates caspase enzymes via adaptor protein ASC for cleaving and activating IL-1β/IL-18 precursor secretion. In a previous study, the CagA virulence factor from *H. pylori* was introduced into gastric mucosal cells, altering the Wnt/β-catenin signaling pathway, thus enhancing the expression of related transcription factors and promoting the sustained high expression of NLRP3 (12). Notably, the expression and activation of the NLRP3 inflammasome can facilitate the proliferation, invasion and metastasis of cancer cells, thereby exerting a notable impact on the initiation and progression of several types of cancer (13,14). NLRP3 is a potent tumor suppressor in colitis-induced colorectal cancer, effectively inhibiting liver metastasis by increasing the anticancer activity of natural killer (NK) cells (15,16). Understanding the potential role of the NLRP3 inflammasome in tumorigenesis and immunomodulation, and its functional mechanism, may reveal relationships with specific types of tumors.

The present study aimed to examine the differential gene expression caused by *H. pylori* infection and the distribution patterns of the NLRP3 inflammasome in GC tissues. The correlation between NLRP3 status and immune cell composition in the tumor microenvironment of GC was also examined, and the effect of NLRP3 on immune infiltration was analyzed to better understand the mechanisms taking place during GC immunotherapy. Additionally, the association between NLRP3 expression levels, immune infiltration and the clinical prognosis of patients with GC was analyzed by integrating data from online public databases and clinical specimens.

Materials and methods

Datasets. The Cancer Genome Atlas (TCGA; https://portal.gdc.cancer.gov/) and Gene Expression Omnibus (GEO; https://www.ncbi.nlm.nih.gov/gds/) databases were used to obtain GC data. The data obtained included gene sequencing and RNA expression data, and relevant clinical information, such as clinical stage, pathological classification and survival status. Cases with incomplete information were excluded from the analysis. A total of 412 sets of clinical data for patients with GC and data from 36 normal tissues were downloaded from TCGA. Among these cases, 157 exhibited *H. pylori* infection, whereas 20 cases showed no evidence of *H. pylori* infection. The primary dataset included patient characteristics such as age, sex, tumor stage, histological grade, initial treatment response, progression-free survival time and overall survival (OS) time. To complement the bioinformatics analysis, a transcriptome dataset from the GEO was obtained (GSE36968) (17) and GSE26253 (18). The majority of GC cases analyzed in the databases mentioned were *H. pylori*-associated GC. The levels of NLRP3 expression among various types of tumors were assessed using TIMER2.0 datasets (19). The association between NLRP3 expression and infiltration of immune cell types in GC was also assessed using NLRP3 expression data obtained from the TIMER2.0 database.

Clinical GC specimens. A total of 65 GC tissues and their adjacent normal tissues were collected from patients diagnosed with GC between May 2018 and June 2023. These patients were recruited from the Gastroscopy Room, Department of Oncology and Radiotherapy, and Department of General Surgery at the Affiliated Changshu Hospital of Nantong University (Changshu, China). GC cases obtained before 2019 were sourced from the biobank established by the hospital. The remaining GC specimens were directly collected from the clinical departments of the hospital. All the patients had provided written informed consent for medical research and were suitable for the study. Out of the 65 patients, 34 were male and 31 were female. The median age was 65.7 years (40.2-81.3 years). All patients with superficial gastritis were identified using gastroscopy. The presence of *H. pylori* infection was verified using a rapid urease test (RUT) (20). GC or precancerous lesions were surgically extracted; two clinically experienced pathologists assessed the histological subtypes and clinical stages based on the World Health Organization classification criteria (21) and pathological test results. Patients

with incomplete standard clinical data, multiple organ failure, another primary tumor or those who had incomplete follow-up data were excluded from the study. Written informed consent for the use of samples for research purposes was obtained from each participant and the Ethics Committee of the Affiliated Changshu Hospital of Nantong University (Changshu Second People's Hospital) approved the study (approval no. 2019-KY-049). Pathological characteristics, including tumor size, tumor location and pathological type were recorded after the initial diagnosis. GC and paracancerous tissues from surgically obtained samples were promptly frozen in liquid nitrogen containers.

NLRP3 mRNA expression levels. NLRP3 mRNA expression levels in clinical samples were quantified by reverse transcription-quantitative PCR. Briefly, total RNA was extracted from GC tissues using TRIzol® Reagent (Invitrogen; Thermo Fisher Scientific, Inc.) according to the manufacturer's protocols. The obtained RNA was reverse-transcribed into cDNA using an RT kit (Cat #. C11027-2; Guangzhou RiboBio Co., Ltd.) at 42˚C for 30 min. TaqMan Gene Expression Assay primers (cat. no. 4331182; Thermo Fisher Scientific, Inc.) were used for NLRP3 (assay ID Hs00918080_g1) and GAPDH (assay ID Hs02786624_g1) expression. In the Hs00918080_g1 assay kit, the forward and reverse primers for NLRP3 were provided as 5'-AGTGGCTGGTGGTGGCTGGT-3' and 5'-CAGGTG CTGCAGGTGCTGC-3', respectively, and qPCR amplification was performed using a Taq Pro Universal SYBR qPCR Master Mix kit (cat. no. Q712-02; Vazyme Biotech Co., Ltd.) under the following conditions: Initial denaturation at 95˚C for 5 min, followed by 35 cycles of denaturation at 95˚C for 30 sec, annealing at 58˚C for 30 sec and extension at 72˚C for 30 sec, with a final extension step at 72˚C for 5 min. All of the reactions were run in triplicate. The cycle quantification (Cq) data were determined using fixed threshold settings. A comparative Cq was used to compare each condition to the control. The relative mRNA expression levels of NLRP3 normalized to the control were calculated with the $2^{-\Delta\Delta Cq}$ method (22).

Association between NLRP3 and pathological characteristics. Kaplan-Meier Plotter (http://www.kmplot.com; n=875 patients with GC) was used to explore the association between NLRP3 expression levels and clinical survival. The results are presented as survival curves showing the hazard ratios (HRs) and P-values were calculated using the log-rank test. The association between NLRP3 expression and the clinical characteristics of patients with GC was conducted using data from the clinical patients.

Acquisition of hub genes. A protein-protein interaction (PPI) network of NLRP3 was constructed using the STRING database (https://www.string-db.org/).

Western blotting. Total protein was extracted from GC specimens using Enhanced RIPA Lysis buffer (cat. no. C5029; BIOSS) and protein concentration was measured using a BCA assay (cat. no. P00105; Beyotime Institute of Biotechnology). Protein samples (40 μg/lane) were separated by SDS-PAGE on an 8% SDS-gel (cat. no. P0012AC; Beyotime Institute of Biotechnology) and were transferred to PVDF membranes (Immobilon®-P; MilliporeSigma). The membranes were then blocked using blocking solution (cat. no. P0023B; Beyotime Institute of Biotechnology) for 1 h at room temperature and then incubated with primary antibodies at 4˚C overnight. The following primary antibodies were used in the present study: Rabbit anti-NLRP3 (1:500; cat. no. ab263899; Abcam) and anti-β-actin (1:1,000; ab8226; Abcam). Subsequently, membranes were washed with TBS-Tween (0.1%) and were incubated with horseradish peroxidase (HRP)-conjugated secondary antibodies (1:5,000; cat. no. TA373083; OriGene Technologies, Inc.) for 1 h at room temperature. Finally, signals were visualized using a BeyoECL Plus kit (cat. no. P00185; Beyotime Institute of Biotechnology) using a ChemiDoc™ MP Imaging system (Bio-Rad Laboratories, Inc.).

Immunohistochemistry (IHC). GC tissues and adjacent normal tissues were fixed in 4% paraformaldehyde at room temperature for 24 h, dehydrated through a graded ethanol series (70, 80, 95 and 100%), cleared in xylene, embedded in paraffin and sectioned into ~4-μm slices. To dewax the tissues, they were immersed in xylene twice (10 min each), followed by hydration for 5 min using a decreasing series of alcohol solutions. Following antigen retrieval using EDTA, endogenous peroxidase activity was quenched using 3% hydrogen peroxide. The cells were then blocked using 1% BSA (cat. no. 0332; Amresco, LLC) at 37˚C for 1 h. Primary anti-human antibodies [NLRP3 (1:500; cat. no. ab263899), CD3 (1:100; cat. no. ab25109), CD4 (1:200; cat. no. ab317787), CD19 (1:500; cat. no. ab245235), CD21 (1:100; cat. no. ab227662) and CD206 (1:500; cat. no. ab64693); all from Abcam] were then added to the tissues and incubated at 4˚C overnight. Subsequently, the tissues were washed three times with PBS (5 min each) and were incubated with HRP-labeled goat anti-rabbit IgG (1:500; cat. no. TA373083; OriGene Technologies, Inc.) and HRP-labeled goat anti-mouse IgG (1:500; cat. no. TA373082; OriGene Technologies, Inc.) at 37˚C for 1 h. The tissues were washed a further three times with PBS (5 min each) and DAB chromogenic solution was used for color development. The nuclei were stained with hematoxylin at 25˚C for 30 min. The staining results were observed under a light microscope, and the areas of positive cell staining were subjected to grayscale analysis (Quantity One 4.62; Bio-Rad Laboratories, Inc.).

RUT. Biopsy specimens of the gastric antrum mucosa, obtained 3-5 cm away from the pylorus during gastroscopy examination, were promptly immersed in RUT detection reagent (Shandong Biomedia Laboratories Co., Ltd.) for 5 min at 37˚C. The change in color of the reagent was directly observed and compared against the corresponding standard. If the phenol red in the reagent transitioned from yellow to red, indicating an elevated pH level, this suggested the presence of *H. pylori* in the tissue, whereas no change in color indicated the absence of *H. pylori*.

Gene enrichment in GC. The R software clusterProfiler package (23) was used to perform Gene Ontology (GO) and KEGG pathway enrichment analysis for TCGA GC database. The median NLRP3 expression levels were used as a threshold to examine the differences in gene enrichment between the groups with high and low NLRP3 expression

based on TCGA database. Gene Set Enrichment Analysis (GSEA; https://www.gsea-msigdb.org/) was performed using the clusterProfiler software package (23). The immune cell gene symbol file (h.all.v2023.2.Hs.symbols.gmt) was obtained from GSEA. Meanwhile KEGG (https://www.kegg.jp/) enrichment analysis was performed on the proteins in the PPI network to identify the pathways associated with the direct interaction targets in the network. Statistical analysis was performed on the functional clustering results and a KEGG pathway enrichment bar chart was generated to visualize the enriched pathways.

Immune cell infiltration and co-expression analysis. The CIBERSORT tool (https://ciberxortx.stanford.edu/) in R studio (version 4.3.1) (24) enables calculations for 22 immune cell proportions in tumor tissues using the inverse convolution approach. Immune cell proportions with $P<0.05$, indicating statistical significance, were included in the subsequent analysis The gastric tumors in TCGA database were classified into high- and low-expression groups using the median NLRP3 mRNA expression level as the threshold. Subsequently, the potential impact of NLRP3 gene expression on the infiltration of immune cells in GC tissues was analyzed. The TIMER2.0 database was used to examine the association between NLRP3 expression and the prevalence of four types of tumor-associated macrophages (macrophage, monocyte, M1 macrophage and M2 macrophage) that infiltrated GC tumors. Co-expression Pearson correlation analysis was performed between NLRP3 and immune checkpoint genes using GC RNA-sequencing (RNA-seq) data from TCGA. The data were analyzed using the R graph visualization software ggplot2 (https://cran.r-project.org/).

Immune infiltration survival analysis. GC RNA-seq data from TCGA were combined with clinical GC tissue data to analyze the relationship between different immune cell infiltrates and patient survival based on the immune cell infiltrates that were significantly influenced by NLRP3. Survival analysis was performed by plotting survival curves for TCGA GC using the survminer package (https://cran.r-project.org/web/packages/survminer/index.html).

Statistical analysis and visualization. R version 4.1.2 was used for bioinformatics analysis. A Wilcoxon rank-sum test was used to evaluate the proportions of immune cell infiltrates in GC tissues between the NLRP3 high-expression and low-expression groups. The NLRP3 expression data were ranked from low to high, and the median of the data was used for statistical calculation of P-values and HR values in survival and survminer packages. All data met the minimum value required for statistical testing (i.e., for data that conforms to a normal distribution, the minimum sample size for each group should be >5). Spearman's correlation analysis was performed to assess the correlation between NLRP3 expression and immune cell infiltrates. GSEA and visualization was performed using clusterProfiler and ggplot2 packages. The Fisher's exact test was performed to analyze the relationship between gene expression levels and clinicopathological parameters. Data are presented as the mean ± SD. Intergroup comparisons were performed using a paired or unpaired Student's t-test, depending on whether the groups were paired or independent. $P<0.05$ was considered to indicate a statistically significant difference.

Results

Expression profile of the NLRP inflammasome in GC. The NLRP family in TCGA datasets consists of a wide variety of inflammasomes. In TCGA, the expression of several NLRP inflammasomes was assessed; specifically, NAIP, NLRC4, NLRP1, NLRP3, NLRP6, NLRP7, NLRP11 and NLRP12. The expression levels of NAIP, NLRC4, NLRP1, NLRP3 and NLRP12 in GC tissues were significantly higher than those in adjacent normal tissues (Fig. 1A). GC datasets (GSE36968 and GSE26253) from the GEO were also analyzed (Fig. 1B and C). GSE36968 included 407 GC tissues and 32 paracancerous tissues, and GSE26253 consisted of 414 GC tissues and 36 paracancerous tissues. Compared with in the paracancerous normal tissues, the expression levels of NLRP3 were significantly greater in GC tissues. Although NLRP3 was not the only upregulated NLRP protein, only NAIP, NLRC4 and NLRP3 were upregulated in GC tissues in both GEO datasets and TCGA datasets. To thoroughly investigate the relationship between NLRP3 and the development of tumors, NLRP3 expression levels in different types of tumors were analyzed. Fig. 1D shows that there were differences in the levels of NLRP3 expression among various types of tumors in TIMER 2.0 datasets. Downregulation of NLRP3 was observed in nine tumor types, namely, bladder urothelial carcinoma, bladder urothelial carcinoma, colon adenocarcinoma, liver hepatocellular carcinoma, pancreatic adenocarcinoma, prostate adenocarcinoma, rectum adenocarcinoma and uterine corpus endometrial carcinoma, compared with in the paracancerous tissues from the patients with cancer. By contrast, increased expression of NLRP3 was observed in head and neck squamous cell carcinoma, renal clear cell carcinoma, kidney renal papillary cell carcinoma and stomach adenocarcinoma (STAD). Further analysis of NLRP3 expression in 10/65 sets of clinical GC tissues and surrounding normal tissues was subsequently performed. Using western blotting, it was demonstrated that the protein expression levels of NLRP3 in GC tissues were higher than in those in normal tissues (Fig. 1E and F). These results indicated that NLRP3 may be significantly upregulated in GC, and could therefore be involved in the development and/or progression of GC.

H. pylori infection promotes NLRP3 expression in GC. A total of 157 cases of GC that tested positive for *H. pylori* infection and 20 cases of GC that tested negative were obtained from the RNA-seq database of TCGA. Fig. 2A shows a comparison and analysis of the differential gene expression between these two groups. Some of the top 50 genes displayed considerable variations in their expression levels. Specifically, certain GC tissues presented increased expression of the NLRP3 gene as a result of *H. pylori* infection. A volcano plot revealed that among the top 10 highly expressed genes in GC tissues positive for *H. pylori* infection, NLRP3 was enriched (Fig. 2B). Furthermore, IHC revealed high expression of NLRP3 in selected clinical GC tissues with *H. pylori* infection (Fig. 2D).

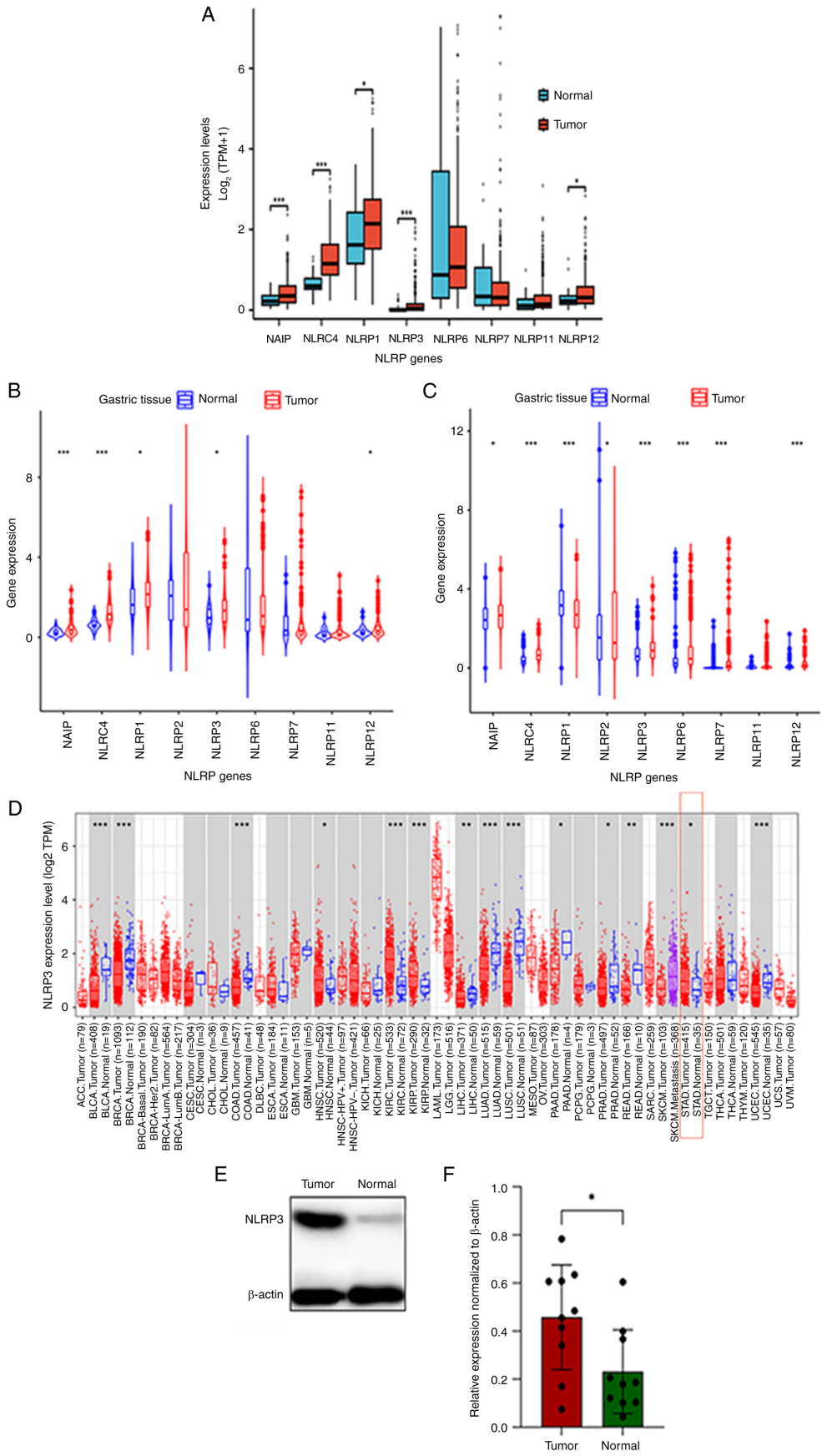

Figure 1. NLRP inflammasome expression profile in GC tumors, and NLRP3 expression levels across several tumor and normal tissues. (A) Expression of the NLRP members in gastric cancer data (STAD) of The Cancer Genome Atlas. Expression of the NLRP members in GC datasets (B) GSE36968 and (C) GSE26253 from Gene Expression Omnibus datasets. (D) Differential expression levels of NLRP3 in different tumors based on data obtained from TIMER2.0 datasets. (E) Representative western blotting results of NLRP3 in tissues from patients with GC. (F) Histogram of NLRP3 expression in samples from 10 patients with GC. *P<0.05, **P<0.01, ***P<0.001. GC, gastric cancer; NLRP, nucleotide-binding oligomerization domain, leucine rich repeat and pyrin domain containing.

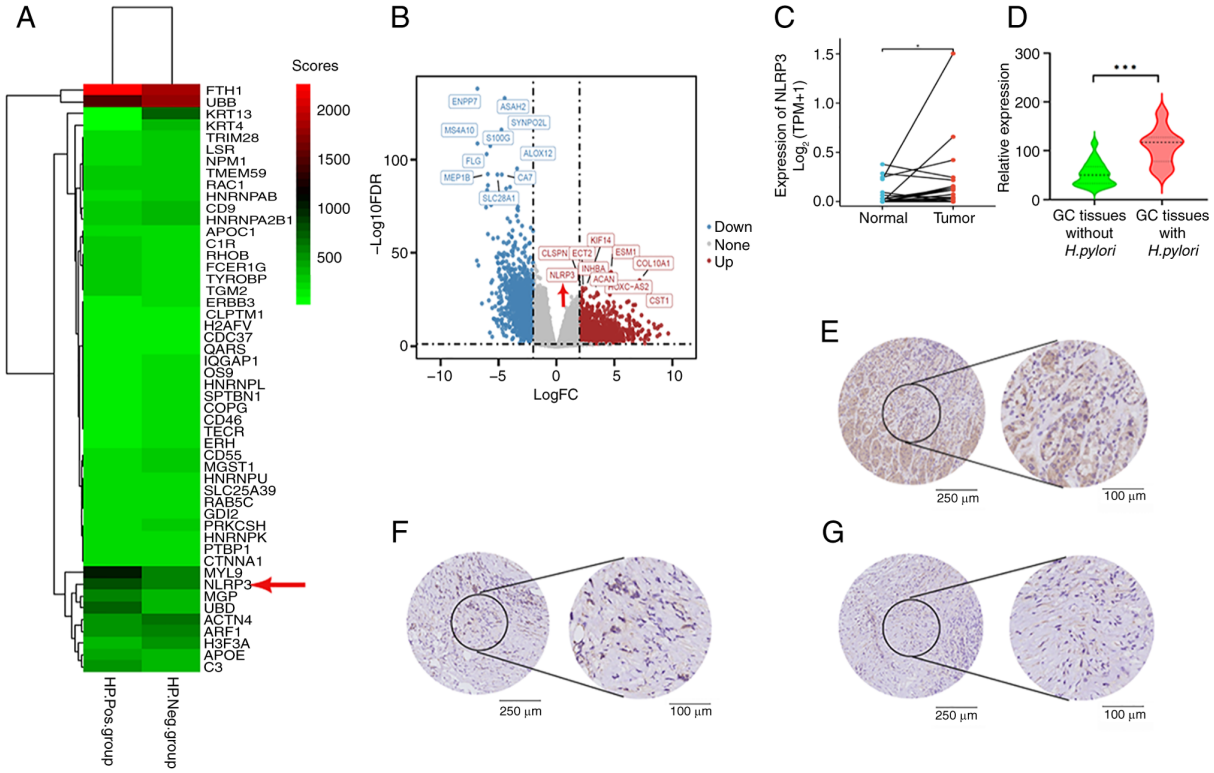

Figure 2. NLRP3 gene expression in GC tissues with or without *Helicobacter pylori* infection. (A) Heatmap of genes associated with *H. pylori* infection in GC tissues from The Cancer Genome Atlas. (B) Volcano plot of differentially expressed genes associated with *H. pylori* infection in GC tissues. (C) mRNA expression levels of NLRP3 in GC and normal tissues. (D) Comparison of NLRP3 expression in GC tissues from patients with *H. pylori* (-) and *H. pylori* (+) GC by IHC. (E) IHC staining of NLRP3 in GC tissues with *H. pylori* infection. (F) IHC staining of NLRP3 in GC tissues without *H. pylori* infection. (G) IHC staining of NLRP3 normal gastric mucosa tissues. *P<0.05, ***P<0.001. FC, fold change; FDR, false discovery rate; GC, gastric cancer; IHC, immunohistochemistry; NLRP, nucleotide-binding oligomerization domain, leucine rich repeat and pyrin domain containing.

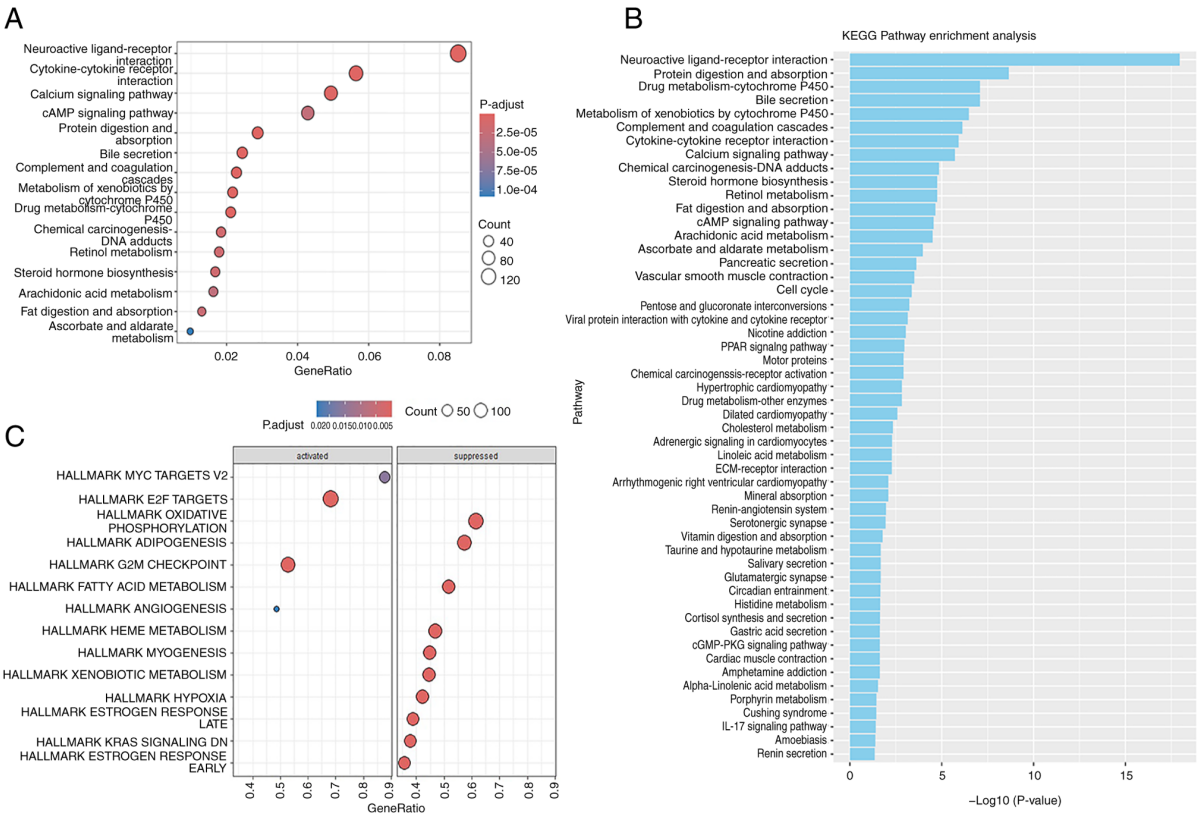

Figure 3. GO and KEGG pathway functional enrichment analyses of genes in gastric cancer tissues. (A) Bubble blot of GO analysis. (B) KEGG pathway enrichment. (C) Gene Set Enrichment Analysis gene pathway enrichment. GO, Gene Ontology; KEGG, Kyoto Encyclopedia of Genes and Genomes.

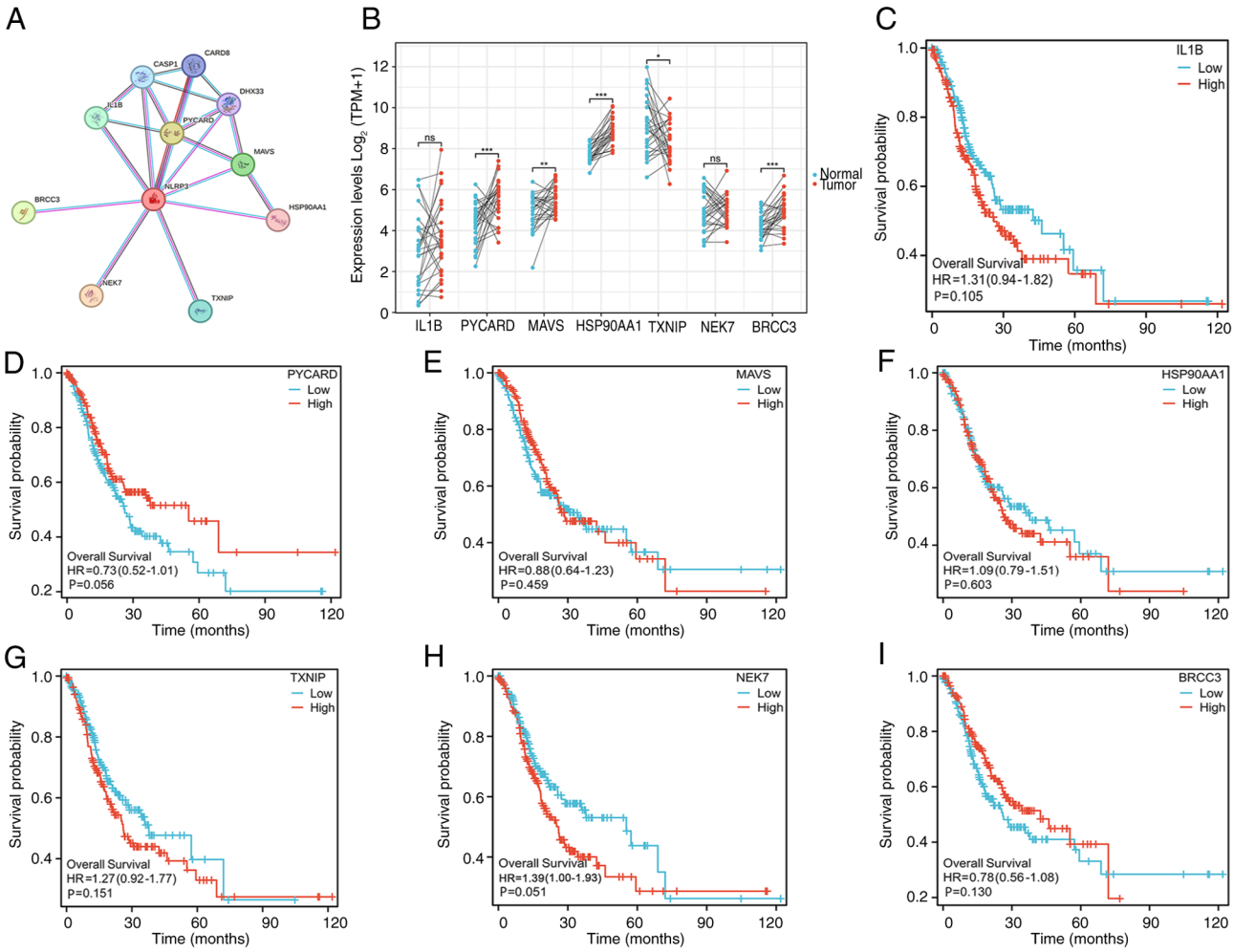

Figure 4. Analysis of hub genes. (A) Protein-protein interaction network of NLRP3. (B) Expression levels of seven related genes in patients with gastric cancer in The Cancer Genome Atlas database. *P<0.05, **P<0.01, ***P<0.001. Survival curve analyses of (C) IL-1B, (D) PYCARD, (E) MAVS, (F) HSP90AA1, (G) TXNIP, (H) NEK7 and (I) BRCC3 genes in gastric cancer. NLRP, nucleotide-binding oligomerization domain, leucine rich repeat and pyrin domain containing; ns, not significant.

Notably, NLRP3 expression was elevated in *H. pylori*-infected GC tissues compared with in uninfected tissues, indicating that *H. pylori* infection might not be the only factor responsible for its upregulation (Fig. 2E-G). Furthermore, examination of NLRP3 mRNA transcription levels in GC tissues revealed a significant increase compared with that in normal gastric mucosa tissues from the same patients (Fig. 2C). The results of IHC consistently revealed considerably high NLRP3 expression in GC tissues infected with *H. pylori* (Fig. 2D).

Functional enrichment analysis of expressed genes in GC. GO analysis revealed that the genes that were expressed in the STAD cohort of patients in TCGA were enriched primarily in pathways related to the interaction between 'Neuroactive ligand-receptor interaction', 'Cytokine-cytokine receptor interaction', 'Calcium signaling pathway' and 'cAMP signaling pathway' (Fig. 3A). GSEA of the differentially expressed genes in GC revealed that the genes were enriched in the MYC, which targets V2, E2F, G2M checkpoint and angiogenesis pathways. Conversely, the top three inhibited pathways included oxidative phosphorylation, adipogenesis and fatty acid metabolism (Fig. 3C). In addition, the KEGG pathway analysis revealed notable enrichment of genes associated with 'Neuroactive ligand-receptor interaction', 'Protein digestion and absorption', 'Drug metabolism-cytochrome P450' and the 'Bile secretion' pathways (Fig. 3B).

Acquisition of the hub genes. The top seven directly related proteins with the highest degree scores were obtained; these were, IL-1B, PYCARD, MAVS, HSP90AA1, TXNIP, NEK7 and BRCC3 (Fig. 4A). These proteins are involved primarily in physiological functions, including infection, inflammation, apoptosis, pyroptosis, innate immunity, transcription regulation, and kinase and cell cycle regulation (25,26). Therefore, NLRP3 may be involved in these important functions. The expression patterns of these proteins in GC in TCGA are shown in Fig. 4B. The expression levels of PYCARD, MAVS, HSP90AA1 and BRCC3 were upregulated in GC tissues. Survival analysis revealed that these seven hub genes were not individually significantly associated with GC prognosis in TCGA dataset (Fig. 4C-I).

Association between NLRP3 expression and clinicopathological parameters. The median of data were calculated for

Table I. Relationships between NLRP3 mRNA expression levels and the clinicopathologic features of patients with gastric cancer.

Clinical feature	Number (%)	NLRP3 mRNA high expression (n=31)	NLRP3 mRNA low expression (n=34)	P-value
Age				0.788
<55 years	18 (27.7)	8	10	
≥55 years	47 (72.3)	23	24	
Sex				0.216
Male	34 (52.3)	19	15	
Female	31 (47.7)	12	19	
Tumor size				>0.999
<5 cm	41 (63.1)	20	21	
≥5 cm	24 (36.9)	11	13	
Lymph node metastasis				0.021[a]
No	38 (58.5)	17	21	
Yes	27 (41.5)	14	13	
TNM stage				<0.0001[a]
I + II	40 (61.5)	11	29	
III + IV	25 (38.5)	20	5	
Pathological type				0.074
Adenocarcinoma	51 (78.5)	20	31	
Others	14 (21.5)	11	3	
Degree of differentiation				0.032[a]
High differentiation	8 (12.3)	2	6	
Moderatedifferentiation	29 (44.6)	11	18	
Low differentiation	28 (43.1)	18	10	
Tumor location				0.116
Gastric antrum	36 (55.4)	16	20	
Entire gastric area	16 (24.6)	11	5	
Others	13 (20.0)	4	9	

[a]P<0.05. NLRP, nucleotide-binding oligomerization domain, leucine rich repeat and pyrin domain containing; TNM, Tumor-Node-Metastasis.

the optimal cut-off value, which was used to split patients into high and low NLRP3 expression. Patients with GC were divided into high expression and low expression groups according to the cut-off value. The Fisher's exact test was conducted to assess the association of NLRP3 expression with clinicopathological characteristics, and no statistically significant differences were identified among patients based on age, sex, pathological type or tumor location (Table I). By contrast, high NLRP3 mRNA expression was significantly associated with poorly differentiated tumors, lymph node metastasis and Tumor-Node-Metastasis (TNM) stage III + IV. These findings indicated that NLRP3 expression may increase as TNM stage progresses with enhanced invasion and metastasis, suggesting an association with the malignant advancement of clinical GC.

Clinical survival and prognostic significance of NLRP3 in GC. The median expression of NLRP3 in GC was used to split patients into high and low NLRP3 expression groups. Kaplan-Meier survival analysis of 875 patients with GC in TCGA database revealed that patients with high levels of NLRP3 expression had significantly lower 5-year OS, progression-free survival and post-progression survival (PPS) rates than those with low expression levels (Fig. 5B-D; OS, HR=1.55, $P=9.3x10^{-7}$; FP, HR=1.61, $P=1.8x10^{-5}$; PPS, HR=2.04, $P=1.9x10^{-9}$). These data indicated a possible link between increased NLRP3 expression and lower survival rates in GC. To verify these findings follow-up data from clinical samples were collected to perform a survival study on a cohort of 65 individuals with GC. The findings revealed a reduced survival rate in individuals with higher NLRP3 expression (Fig. 5A), in agreement with the aforementioned results. Thus, constitutively high levels of NLRP3 expression may be associated with a worse prognosis in patients with GC.

NLRP3 affects the infiltration of different types of immune cells. CIBERSORT was used to examine the presence of 22 immune cell types in tissues. Analysis revealed that in the GC group, the presence of regulatory T cells (Tregs), M0 macrophages, naïve B cells, T helper (Th) cells, M1 macrophages, activated mast cells and memory-activated $CD4^+$ T cells was significantly higher

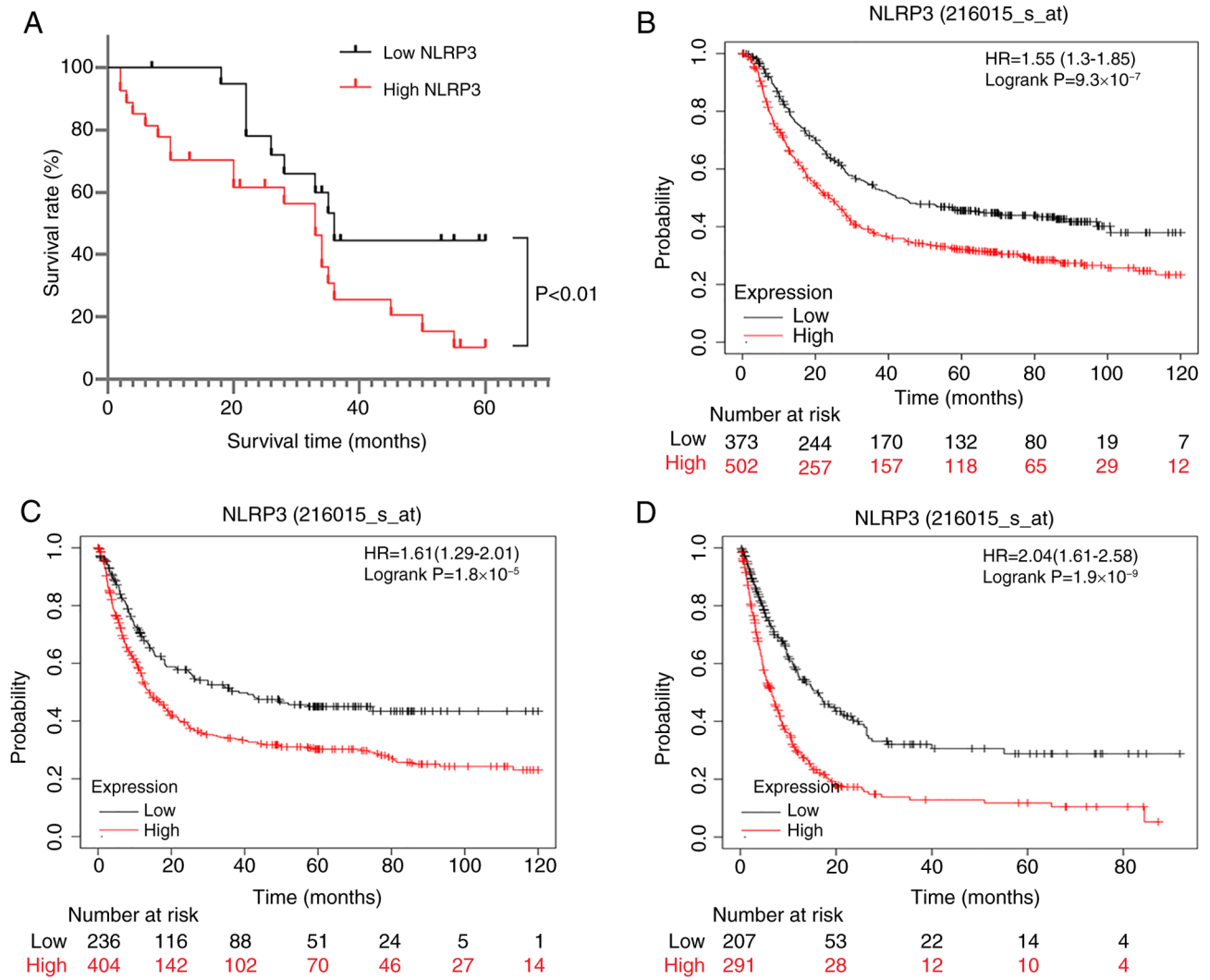

Figure 5. Survival curves of patients with high and low NLRP3 expression in GC. (A) A 5-year OS curve of patients with GC. (B) Upregulated expression of NLRP3 in the Kaplan-Meier Plotter database was associated with a worse 10-year OS. (C) Progression-free survival and (D) post-progression survival analysis based on NLRP3 expression using the Kaplan-Meier Plotter database. GC, gastric cancer; NLRP, nucleotide-binding oligomerization domain, leucine rich repeat and pyrin domain containing; OS, overall survival.

in GC compared with in normal tissues (Fig. 6A). By contrast, the presence of plasma cells, resting mast cells and monocytes was significantly reduced in tumor tissues. Regarding the distribution of immune cells within the tumor, the majority of immune cells were $CD8^+$ T cells and resting memory $CD4^+$ T cells, followed by M2 macrophages, Tregs, M0 macrophages, plasma cells and naïve B cells (Fig. 6B). Correlation analysis was performed to examine the relationship between immune cell ratios in GC tissues. The results revealed a strong negative association between $CD8^+$ T cells and resting memory $CD4^+$ T cells (Fig. 6C). Conversely, there was a positive correlation between M1 macrophages and each of the following: Active memory $CD4^+$ T cells, $CD8^+$ T cells and T cells follicular helper (Fig. 6C). Furthermore, high expression of NLRP3 in GC was positively correlated with activated mast cells, resting NK cells, M2 macrophages and neutrophils, whereas it exhibited negative correlation with Tregs, CD8 T cells, activated NK cells and follicular helper T cells (Fig. 6D). Additionally, there was a positive correlation between NK cells and M2 macrophages; conversely, there was a negative correlation with Tregs and $CD8^+$ T cells (Fig. 6C).

GSEA of GC immune signaling pathways associated with NLRP3. GSEA was used to examine the immune gene expression sets specifically associated with NLRP3 in GC. The data were split into two categories (high and low) based on median NLRP3 expression levels. GSEA revealed that GC tissues with high NLRP3 expression exhibited a notable enrichment in the oxidative phosphorylation signaling pathway, E2F signaling pathway (Fig. 7A). The expression of NLRP3 suppressed oxidative phosphorylation, with the primary activation routes being E2F signaling and G2M checkpoint signaling (Fig. 7B); the activating and inhibitory effects of NLRP3 in the two signaling pathways are shown in Fig. 7C (the red line represents the E2F signaling pathway activated by NLRP3, and the blue line represents oxidative phosphorylation signaling inhibited by NLRP3). The E2F target gene set was activated, whereas the oxidative phosphorylation gene set was inhibited. The mountain range map (Fig. 7D) and bubble plot (Fig. 7E) show that NLRP3 mostly affected gene activities related to ribosomes, olfactory transduction and insulin secretion.

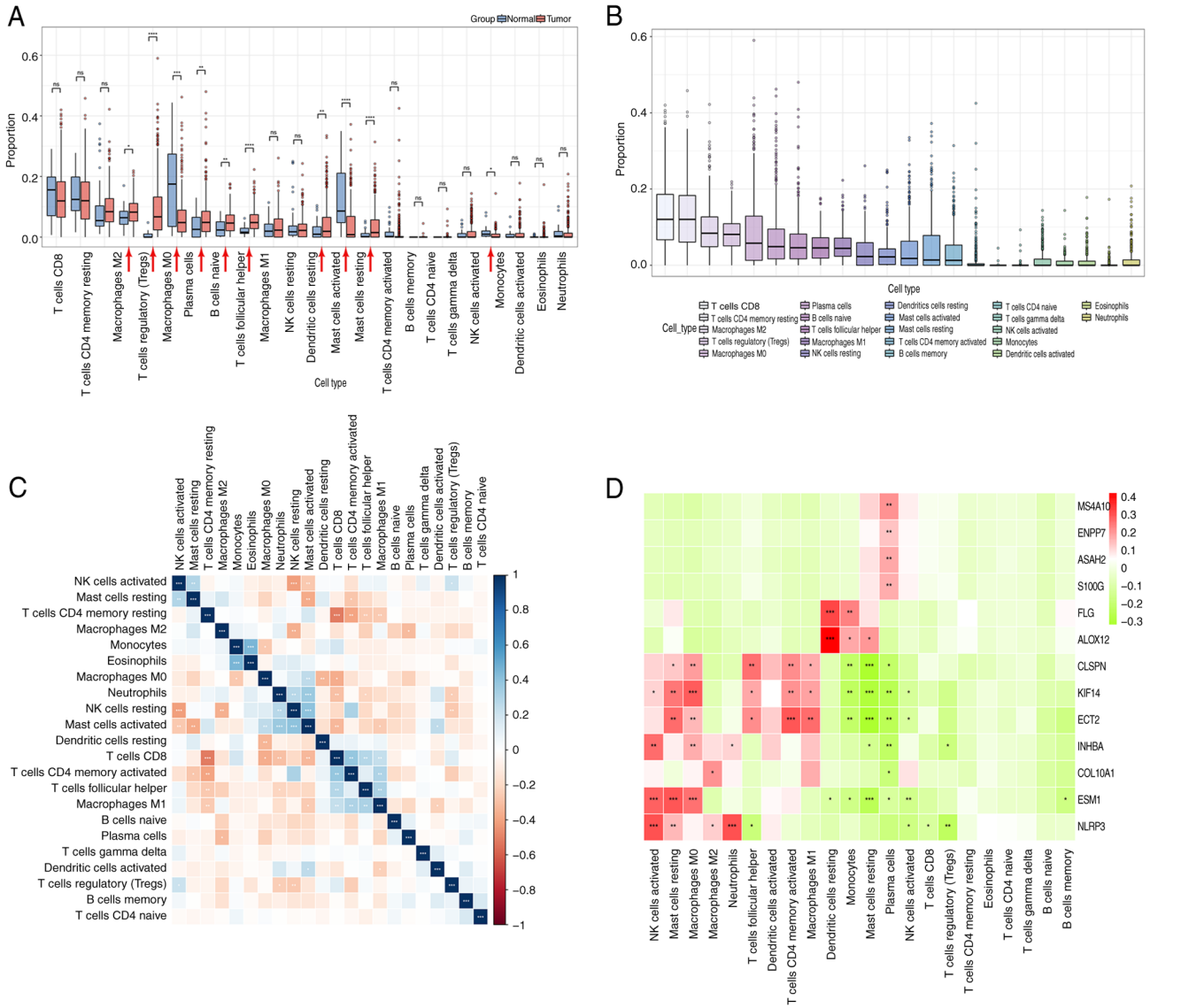

Figure 6. Results of CIBERSORT analysis on the infiltration of different immune cells affected by NLRP3 expression in GC tissues. (A) Proportion of immune infiltration in GC tumor tissues vs. normal tissues. (B) Box plot of the proportions of immune cells in GC tissues. (C) Heatmap of the correlation of different immune cell infiltrates in GC tissues. Blue indicates a positive correlation, and red indicates a negative correlation. (D) Types of immune cell infiltrates primarily affected by NLRP3 and other genes. Red indicates a positive correlation and indicates a negative correlation. *P<0.05, **P<0.01, ***P<0.001. GC, gastric cancer; NLRP, nucleotide-binding oligomerization domain, leucine rich repeat and pyrin domain containing.

Relationship between NLRP3 and immune cell checkpoints. The relationship between NLRP3 expression and 57 immune cell markers in GC was analyzed to investigate the possible mechanisms by which NLRP3 regulated the infiltration of immune cells. The expression of NLRP3 in innate immune cells was strongly positively associated with various indicators of monocytes, tumor-associated macrophages (TAMs), M2 macrophages, neutrophils and dendritic cells. The correlation coefficients for all these markers were between 0.424 and 0.746 and the P-values were all <0.0001 (Fig. 8A). Specifically, the expression levels of NLRP3 were strongly positively associated with the expression levels of programmed cell death-1 (PDCD1) (r=0.453), cytotoxic T-lymphocyte antigen 4 (CTLA4; r=0.506), lymphocyte activation 3 (LAG3) (r=0.433), and T-cell immunoglobulin, and mucin structural domain-containing protein 3 (TIM-3; r=0.720) (P<0.0001; Fig. 8B); These markers serve a role in immune checkpoints. The co-expression heatmap of each single gene revealed consistent findings (Fig. 8B).

NLRP3 is involved in macrophage polarization. The levels of NLRP3 expression were weakly correlated with M1 macrophages in GC tissues, and strongly correlated with M2 macrophages, TAMs and monocytes (Fig. 9A-D). This suggested that NLRP3 may serve a role in promoting the polarization of TAMs towards the M2 phenotype. The aforementioned findings strongly indicated that NLRP3 may have a role in the regulation of immune cell infiltration in GC.

Immune infiltration of T lymphocytes and macrophages in clinical GC tissues. Examination of immune infiltration revealed that increased expression of NLRP3 led to a higher presence of $CD8^{+}$ T cells, $CD4^{+}$ resting memory T cells, M2 macrophages and Tregs in GC tissues (Fig. 6B). Conversely,

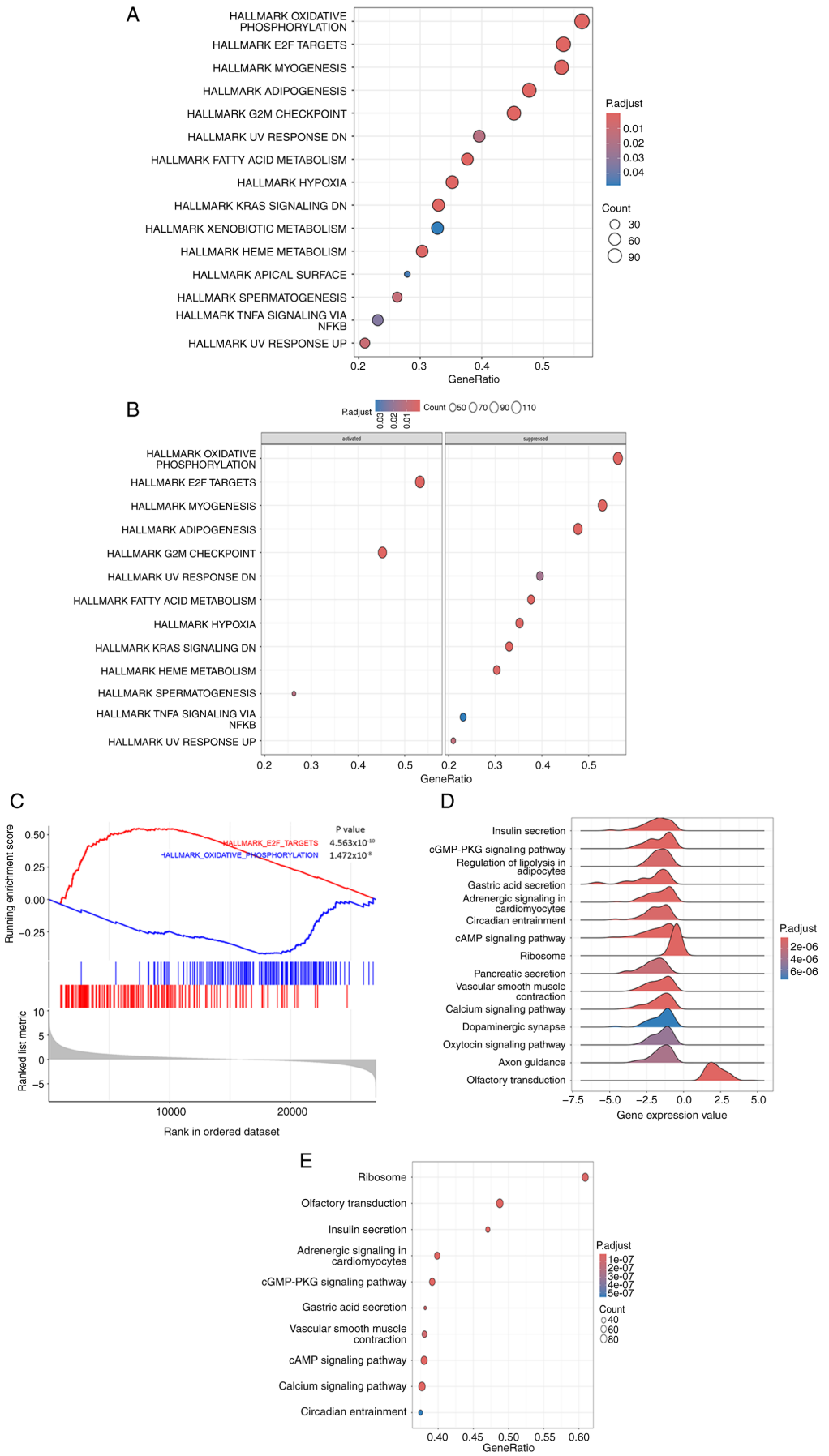

Figure 7. GSEA of NLRP3-influenced gene signaling function pathways in gastric cancer tissues. (A) Top 15 signaling pathways significantly affected by NLRP3. (B) Signaling pathways activated and suppressed by NLRP3. (C) GSEA of signaling pathways activated (E2F targets gene set) or inhibited (oxidative phosphorylation gene set) by NLRP3. (D) NLRP3 GSEA mountain range maps. (E) NLRP3 GSEA bubble plots. GSEA, Gene Set Enrichment Analysis; NLRP, nucleotide-binding oligomerization domain, leucine rich repeat and pyrin domain containing.

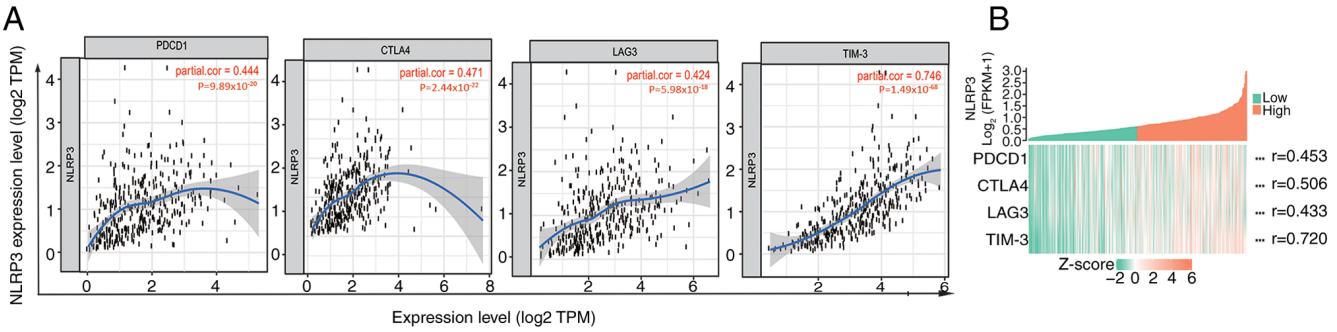

Figure 8. Correlation of NLRP3 with immune checkpoints. (A) Scatterplots showing the correlation between immune checkpoint genes and NLRP3 expression. (B) Single gene co-expression heat map of NLRP3 with immune checkpoint genes. ***P<0.001. NLRP, nucleotide-binding oligomerization domain, leucine rich repeat and pyrin domain containing.

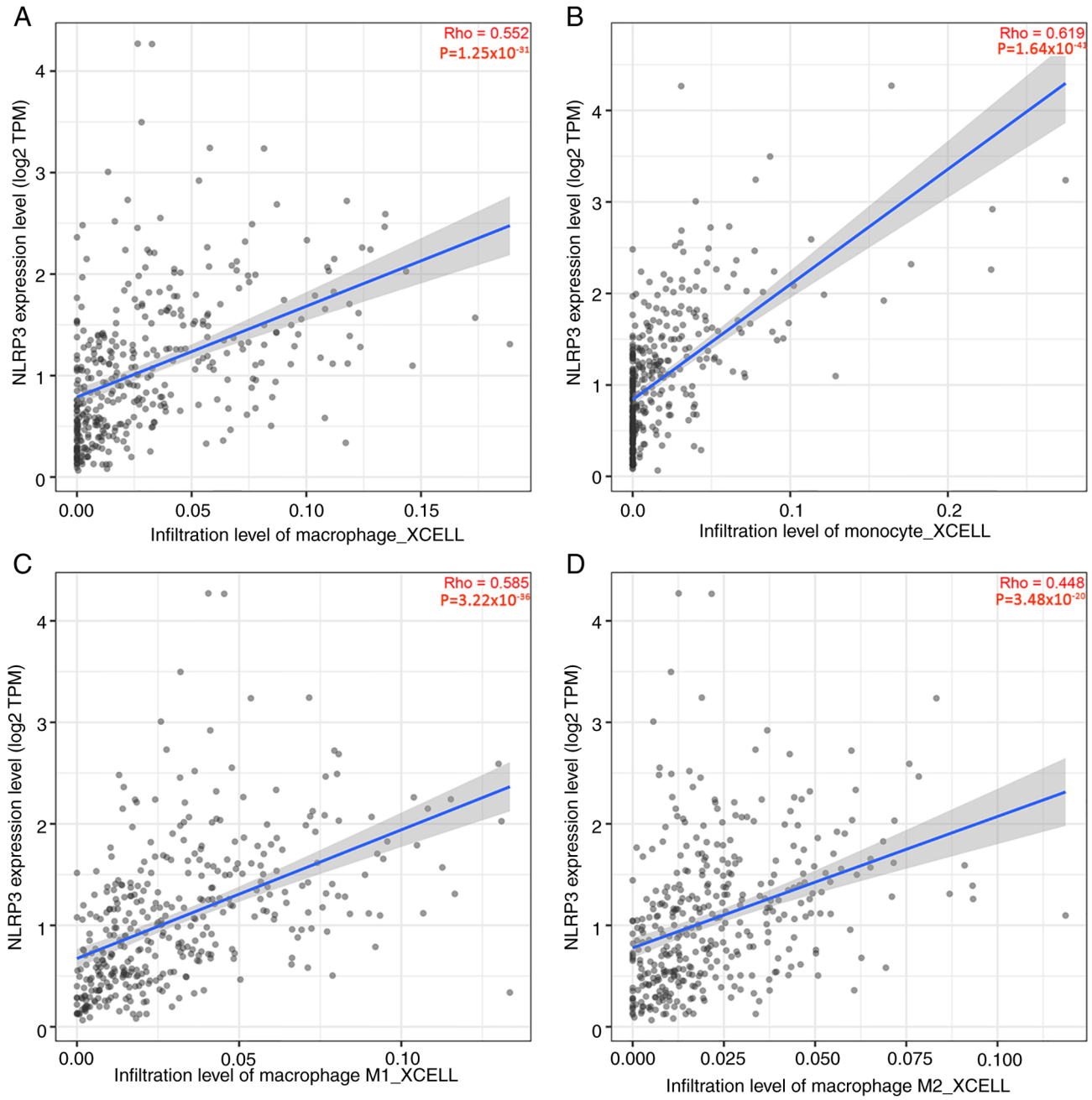

Figure 9. NLRP3 expression levels and macrophage polarization in gastric cancer. Scatter plots of (A) tumor-associated macrophage, (B) monocyte, (C) M1 macrophage and (D) M2 macrophage infiltration levels based on NLRP3 expression. NLRP, nucleotide-binding oligomerization domain, leucine rich repeat and pyrin domain containing.

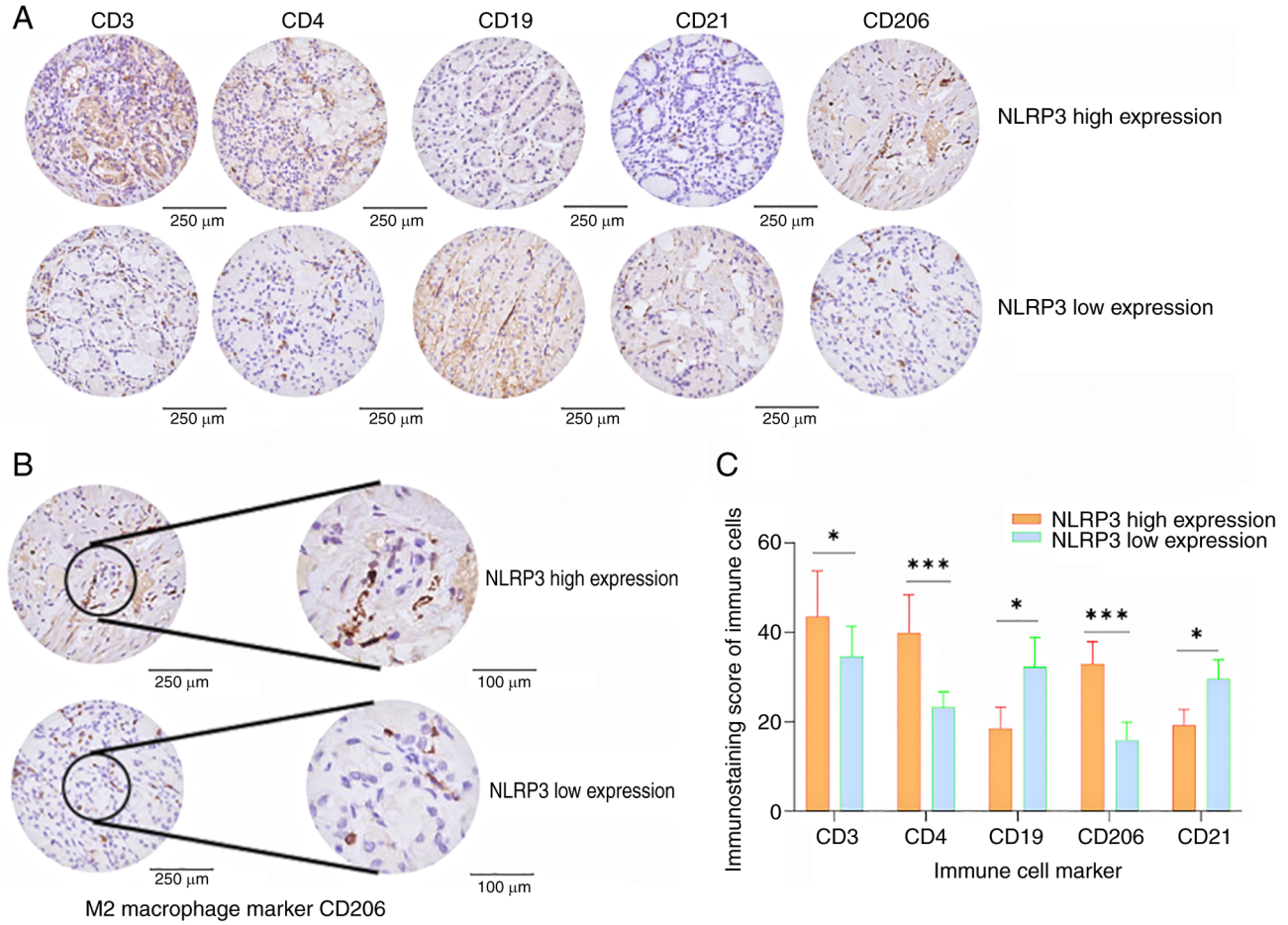

Figure 10. High NLRP3 expression promotes immune cell infiltration. (A) Representative IHC staining images of immune cell surface markers. (B) Enlarged IHC image of the M2 macrophage marker CD206. (C) Histogram of immunohistochemical cell count scores. *P<0.05, ***P<0.001. NLRP, nucleotide-binding oligomerization domain, leucine rich repeat and pyrin domain containing; IHC, immunohistochemistry.

the levels of Tregs, follicular Th cells and M1 macrophages were higher in GC tissues compared with in normal tissues (Fig. 6A). Based on the median NLRP3 score, the 65 cases of GC were categorized into high and low expression groups. Comparing the immune cell counts in the two groups revealed that the GC tissues with high NLRP3 expression had significantly higher counts of $CD3^+$, $CD4^+$ and $CD206^+$ cells compared with those in the low NLRP3 expression group (Fig. 10). Conversely, the counts of $CD19^+$ and $CD21^+$ cells were lower in the high NLRP3 expression group. Representative IHC images are shown in Fig. 10A and B; and comparative analysis between the target immune cell marker scores is shown in Fig. 10C.

Immune infiltration survival analysis. The survminer software package was used to plot and analyze survival curves. The proportion of CD3D (a component of the CD3 complex) and CD206 cell infiltration had a significant effect on the survival of patients with GC. Patients with a high percentage of T lymphocytes with high CD3D expression had a significantly greater survival rate compared with those with a low percentage (Fig. 11A). However, patients with a high percentage of M2 macrophage infiltration (high CD206 expression) had a lower survival rate (Fig. 11F). There was no significant relationship between the proportion of infiltration of other types of immune cells (CD4, CD8, CD80 and CD19) and survival rate (Fig. 11B-E).

Discussion

In the present study, NLRP3 expression exhibited marked variation based on cancer type. The NLRP proteins are implicated in various cellular physiological functions, with distinct mechanisms attributed to different members across different tissues and/or diseases (27,28). The protein expression of NLRPs varies across different types of tumors, necessitating further investigation into the underlying mechanisms (14). In the current study, the aberrant upregulation of NLRP3 has been observed in GC tissues, which could be attributed to persistent *H. pylori* infection. NLRP3 upregulation was observed in GC tissues collected from patients, and this upregulation was associated with the malignant degree of GC. In addition, elevated NLRP3 expression was associated with distant metastases. Upregulated expression of NLRP3 was also predictive of an unfavorable prognosis for patients with GC. Notably, there was a positive association between NLRP3 expression and lymph node metastasis, infiltration and distant metastasis, which is in agreement with a previous pan-cancer analysis of NLRP3 (29).

NLRP3 may participate in the regulation of infection-induced inflammatory receptor ligands and the

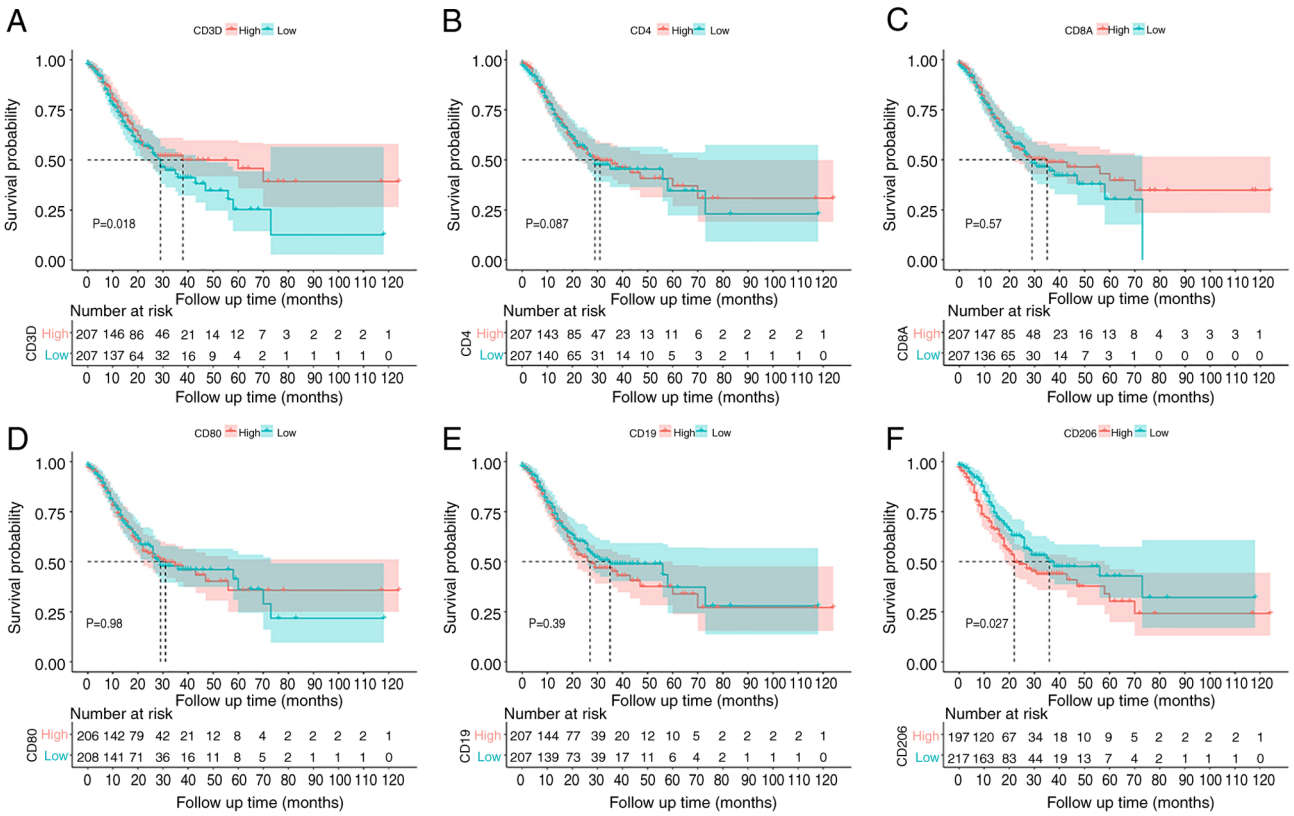

Figure 11. Survival curve analysis of patients with different immune cell markers in gastric cancer. Association of (A) $CD3^+$ regulatory T cell, (B) $CD4^+$ T lymphocyte, (C) $CD8^+$ cytotoxic lymphocyte, (D) $CD80^+$ M1 macrophage, (E) $CD19^+$ B lymphocyte and (F) $CD206^+$ M2 macrophage cell infiltration with survival.

modulation of cellular inflammatory factors. The tumor microenvironment secretes various factors that regulate tumor behavior (30), and inflammation may act as a defense mechanism against cancer cells, with inflammasomes serving a pivotal role in tumor progression, prognosis and treatment response (31,32). Research has demonstrated the benefits of utilizing the immune system to combat tumors, as opposed to conventional treatments (33). The immune cell makeup in cancer tissues can reveal promising targets for cancer therapy that may be utilized to modulate the immune system and effectively combat cancer cells (34,35).

In the present study, patients with GC with a high degree of macrophage infiltration experienced a significant decrease in survival. Furthermore, NLRP3 was positively correlated with Tregs, and it has been suggested that NLRP3 may stimulate the production of Tregs. It could be hypothesized that increased NLRP3 expression may lead to enhanced infiltration of T lymphocytes, particularly Tregs, and can promote the transformation of macrophages from an M1 to an M2 phenotype. $CD3^+$ T cells are widely hypothesized to possess antitumor properties, and substantial infiltration of $CD3^+$ T cells is indicative of a favorable prognosis for patients with GC (36). $CD4^+$ T lymphocytes consist of four distinct groups: Th1, Th2, Th17 and Treg cells (37). Th1 and Th2 cells have the potential to contribute to the suppression of tumor cells, and the extent of their infiltration is directly proportional to the benefits of immunotherapy for patients with GC (37,38). In addition, $CD4^+$ T cells primarily exert antitumor actions; however, the impact of $CD8^+$ T cells on tumor cells is contingent upon the specific condition (39). A previous study demonstrated that the presence of Tregs and M2 macrophages in GC tissues can positively influence the effectiveness of antitumor treatment (40). In the current study, patients with GC who exhibited high expression levels of CD3D in their tumor tissues demonstrated a significantly higher survival rate, whereas those with elevated levels of CD206 and a high infiltration of M2 macrophages showed a lower survival rate.

TAMs are mostly identified using CD68 as their major marker (41). The distribution of TAMs differs across different types of cancer, and different types of TAMs can have either anticancer or pro-cancer effects (42). Research has indicated that TAMs may function as promoters of cancer during tumor growth (43). Upregulation of NLRP3 in GC tissues has been shown to lead to the polarization of macrophages towards an M2 phenotype, which promotes the development of cancer. NLRP3 may also lead to the activation of caspase-1, and the production of IL-1β and IL-18 cytokines, which may facilitate the transformation of immune cell infiltration (44).

B cells have been hypothesized to develop a range of antibodies and to enhance the function of T cells, which allows the body to combat foreign antigens from viral and bacterial infections (45). The association between the functional enrichment of genes and immune cell infiltration in cancer is intricate. Upregulated expression of NLRP3 was shown to be associated with the enrichment of cell cycle-related gene sets (E2F targets and G2M checkpoint), which are associated with ribosomes, olfactory transduction and insulin secretion.

Tumor immunotherapy employs immune checkpoint inhibitors to restore antitumor immune responses by activating co-suppressive T-cell signaling. This therapy has demonstrated significant clinical effectiveness in several types of cancer (46,47). In the present study, a favorable correlation between NLRP3 and the immune checkpoint genes TIM-3, PDCD1, CTLA4 and LAG3 was identified. TIM-3 has a crucial role in controlling the function of dendritic cells and limiting the immunological response to tumors by regulating activation of the NLRP3 inflammasome (48). The NLRP3 inflammasome increases the expression of PD-L1 and contributes to the inhibition of the immune response in lymphoma (49). Thus, based on the findings of previous studies, NLRP3 may regulate immunological checkpoints and facilitate the immune system evasion of tumor cells.

In the present study, the function of NLRP3 as a prognostic marker of GC was assessed and the results showed an association between NLRP3 and immune cell infiltration in GC. NLRP3 exhibits contrasting effects in the tumor microenvironment of GC, exhibiting distinct pro- and anticancer effects through immune cell infiltration. By reducing the infiltration ratio of M1/M2 macrophages, cancer progression is promoted, whereas increasing the M1/M2 ratio can exert anticancer effects. By targeting NLRP3, the immune cell infiltration pattern in GC tissues may be manipulated to improve patient outcomes. By stimulating the infiltration of immune cells to shift from inhibiting tumor immune evasion to promoting antitumor effects, it could be possible to suppress the proliferation and migration of GC cells. Modulating NLRP3 levels by interfering with protein expression, such as via antibody-based drug inhibition, genetic interference and inflammation control, could prevent NLRP3 inflammation-related diseases, including GC. However, completely blocking NLRP3 may also lead to notable side effects, as it would eliminate the beneficial roles of NLRP3 inflammation in eliminating harmful pathogens (50). Developing precise and efficient methods that appropriately block the inflammatory activity of the NLRP3 inflammasome may serve as a novel strategy and approach for preventing and treating GC.

The present study has some limitations. Databases provided by different research centers may have differences in research methodologies and experimental outcomes. Although statistical methods minimized the bias, the heterogeneity of the data can hinder the reproducibility of the findings to some extent. Increasing the sample size and extending the follow-up period may allow for a more accurate assessment of prognostic value. The detailed mechanisms by which NLRP3 regulates immune infiltration in GC require further research. NLRP3 may serve as a prognostic marker for GC; however, the practicality and effectiveness of assessing its expression in different clinical contexts remain to be confirmed. The heterogeneity among individuals with GC may also affect its general applicability as a prognostic marker.

In conclusion, the results of the present study showed that NLRP3 expression was upregulated in GC tissues compared with in normal tissues from TCGA dataset; this finding was confirmed in clinical samples. Higher NLRP3 expression was demonstrated to promote the progression of larger tumors with lymph node metastasis, advanced TNM stages or poor differentiation. NLRP3 was revealed to be associated with NK cells and M2 macrophages, and to be inversely correlated with Tregs and $CD8^+$ T cells. Furthermore, high NLRP3 expression led to increased $CD3^+$, $CD4^+$ and $CD206^+$ cell infiltration, which may regulate cancer cell proliferation and migration, ultimately leading to an unfavorable prognosis in patients with GC.

Acknowledgements

Not applicable.

Funding

This study was supported by grants from the Medical Research Support Project of Changshu Health Committee (grant no. CSWS202106), the Changshu Science and Technology Program Project (grant no. CS202018), the Basic Research Program-Medical Application Basic Research Project (grant no. CY202330) and Suzhou Science and Technology Bureau Clinical Trial Institution Capacity Improvement Project (SLT2023007).

Availability of data and materials

The data generated in the present study may be requested from the corresponding author.

Authors' contributions

CW, YX and YG conceived the project. PW, YZ and XC collected specimens and performed experiments. CW, YX and PW conducted the experiments. YX, PW and YZ analyzed the data. CW and PW drafted the manuscript. PW, YX and YG confirm the authenticity of all the raw data. All authors read and approved the final version of the manuscript.

Ethics approval and consent to participate

The study was conducted in accordance with The Declaration of Helsinki, and was approved by the Ethics Committee of Affiliated Changshu Hospital of Nantong University (approval no. 2019-KY-049). Written informed consent for the use of samples for research purposes was obtained from each participant.

Patient consent for publication

All patients provided written informed consent for the publication of medical research findings.

Competing interests

The authors declare that they have no competing interests.

References

1. Heuvers ME, Wisnivesky J, Stricker BH and Aerts JG: Generalizability of results from the national lung screening trial. Eur J Epidemiol 27: 669-672, 2012.
2. Billan S, Kaidar-Person O and Gil Z: Treatment after progression in the era of immunotherapy. Lancet Oncol 21: e463-e476, 2020.

3. Shaopeng Z, Yang Z, Yuan F, Chen H and Zhengjun Q: Regulation of regulatory T cells and tumor-associated macrophages in gastric cancer tumor microenvironment. Cancer Med 13: e6959, 2024.
4. Zhai Y, Liu X, Huang Z, Zhang J, Stalin A, Tan Y, Zhang F, Chen M, Shi R, Huang J, *et al*: Data mining combines bioinformatics discover immunoinfiltration-related gene SERPINE1 as a biomarker for diagnosis and prognosis of stomach adenocarcinoma. Sci Rep 13: 1373, 2023.
5. Kao KC, Vilbois S, Tsai CH and Ho PC: Metabolic communication in the tumour-immune microenvironment. Nat Cell Biol 24: 1574-1583, 2022.
6. Chen F, Chen N, Gao Y, Jia L, Lyu Z and Cui J: Clinical progress of PD-1/L1 inhibitors in breast cancer immunotherapy. Front Oncol 11: 724424, 2022.
7. Chen X, Zhang W, Yang W, Zhou M and Liu F: Acquired resistance for immune checkpoint inhibitors in cancer immunotherapy: Challenges and prospects. Aging (Albany NY) 14: 1048-1064, 2022.
8. Wen H, Miao EA and Ting JP: Mechanisms of NOD-like receptor-associated inflammasome activation. Immunity 39: 432-441, 2013.
9. Mitchell PS, Sandstrom A and Vance RE: The NLRP1 inflammasome: New mechanistic insights and unresolved mysteries. Curr Opin Immunol 60: 37-45, 2019.
10. Kufer TA and Sansonetti PJ: NLR functions beyond pathogen recognition. Nat Immunol 12: 121-128, 2011.
11. Arfsten H, Cho A, Prausmüller S, Spinka G, Novak J, Goliasch G, Bartko PE, Raderer M, Gisslinger H, Kornek G, *et al*: Inflammation-based scores as a common tool for prognostic assessment in heart failure or cancer. Front Cardiovasc Med 8: 725903, 2021.
12. Yong X, Tang B, Li BS, Xie R, Hu CJ, Luo G, Qin Y, Dong H and Yang SM: *Helicobacter pylori* virulence factor CagA promotes tumorigenesis of gastric cancer via multiple signaling pathways. Cell Commun Signal 13: 30, 2015.
13. Hu Q, Zhao F, Guo F, Wang C and Fu Z: Polymeric nanoparticles induce NLRP3 inflammasome activation and promote breast cancer metastasis. Macromol Biosci 17: 1700273, 2017.
14. Zhang X, Li C, Chen D, He X, Zhao Y, Bao L, Wang Q, Zhou J and Xie Y: *H. pylori* CagA activates the NLRP3 inflammasome to promote gastric cancer cell migration and invasion. Inflamm Res 71: 141-155, 2022.
15. Allen IC, TeKippe EM, Woodford RM, Uronis JM, Holl EK, Rogers AB, Herfarth HH, Jobin C and Ting JP: The NLRP3 inflammasome functions as a negative regulator of tumorigenesis during colitis-associated cancer. J Exp Med 207: 1045-1056, 2010.
16. Dupaul-Chicoine J, Arabzadeh A, Dagenais M, Douglas T, Champagne C, Morizot A, Rodrigue-Gervais IG, Breton V, Colpitts SL, Beauchemin N and Saleh M: The Nlrp3 inflammasome suppresses colorectal cancer metastatic growth in the liver by promoting natural killer cell tumoricidal activity. Immunity 43: 751-763, 2015.
17. Chang HR, Nam S, Kook MC, Kim KT, Liu X, Yao H, Jung HR, Lemos R Jr, Seo HH, Park HS, *et al*: HNF4α is a therapeutic target that links AMPK to WNT signalling in early-stage gastric cancer. Gut 65: 19-32, 2016.
18. Oh SC, Sohn BH, Cheong JH, Kim SB, Lee JE, Park KC, Lee SH, Park JL, Park YY, Lee HS, *et al*: Clinical and genomic landscape of gastric cancer with a mesenchymal phenotype. Nat Commun 9: 1777, 2018.
19. Li T, Fan J, Wang B, Traugh N, Chen Q, Liu JS, Li B and Liu XS: TIMER: A web server for comprehensive analysis of tumor-infiltrating immune cells. Cancer Res 77: e108-e110, 2017.
20. Elbehiry A, Marzouk E, Aldubaib M, Abalkhail A, Anagreyyah S, Anajirih N, Almuzaini AM, Rawway M, Alfadhel A, Draz A and Abu-Okail A: *Helicobacter pylori* infection: Current status and future prospects on diagnostic, therapeutic and control challenges. Antibiotics (Basel) 12: 191, 2023.
21. Kushima R: The updated WHO classification of digestive system tumours gastric adeno-carcinoma and dysplasia. Pathologe 43: 8-15, 2022.
22. Livak KJ and Schmittgen TD: Analysis of relative gene expression data using real-time quantitative PCR and the 2(-Delta Delta C(T)) method. Methods 25: 402-408, 2001.
23. Yu G, Wang LG, Han Y and He QY: clusterProfiler: An R package for comparing biological themes among gene clusters. OMICS 16: 284-287, 2012.
24. RStudio Team. RStudio: Integrated Development for R. RStudio, Inc., Boston, MA, 2015. http: //www.rstudio.com/.
25. Ghazi BK, Bangash MH, Razzaq AA, Kiyani M, Girmay S, Chaudhary WR, Zahid U, Hussain U, Mujahid H, Parvaiz U, *et al*. In silico structural and functional analyses of NLRP3 inflammasomes to provide insights for treating neurodegenerative diseases. Biomed Res Int 23: 9819005, 2023.
26. An S, Li X, Li B and Li Y: Comprehensive analysis of epigenetic associated genes with differential gene expression and prognosis in gastric cancer. Comb Chem High Throughput Screen 26: 527-538, 2023.
27. Shen Y, Qian L, Luo H, Li X, Ruan Y, Fan R, Si Z, Chen Y, Li L and Liu Y: The significance of NLRP inflammasome in neuropsychiatric disorders. Brain Sci 12: 1057, 2022.
28. Moon SW, Son HJ, Mo HY, Yoo NJ and Lee SH: Somatic mutation of NLRP genes in gastric and colonic cancers. Pathol Oncol Res 27: 607385, 2021.
29. Shadab A, Mahjoor M, Abbasi-Kolli M, Afkhami H, Moeinian P and Safdarian AR: Divergent functions of NLRP3 inflammasomes in cancer: A review. Cell Commun Signal 21: 232, 2023.
30. Kim J and Bae JS: Tumor-associated macrophages and neutrophils in tumor microenvironment. Mediators Inflamm 2016: 6058147, 2016.
31. Bruchard M, Mignot G, Derangère V, Chalmin F, Chevriaux A, Végran F, Boireau W, Simon B, Ryffel B, Connat L, *et al*: Chemotherapy-triggered cathepsin B release in myeloid-derived suppressor cells activates the Nlrp3 inflammasome and promotes tumor growth. Nat Med 19: 57-64, 2013.
32. Karki R and Kanneganti TD: Diverging inflammasome signals in tumorigenesis and potential targeting. Nat Rev Cancer 19: 197-214, 2019.
33. Lin C, He H, Liu H, Li R, Chen Y, Qi Y, Jiang Q, Chen L, Zhang P, Zhang P, *et al*: Tumour-associated macrophages-derived CXCL8 determines immune evasion through autonomous PD-L1 expression in gastric cancer. Gut 68: 1764-1773, 2019.
34. Huo J, Wu L and Zang Y: Development and validation of a robust immune-related prognostic signature for gastric cancer. J Immunol Res 2021: 5554342, 2021.
35. Tang X, Guo T, Wu X, Gan X, Wang Y, Jia F, Zhang Y, Xing X, Gao X and Li Z: Clinical significance and immune infiltration analyses of the cuproptosis-related human copper proteome in gastric cancer. Biomolecules 12: 1459, 2022.
36. Du Z, Xiao Y, Deng G, Song H, Xue Y and Song H: CD3+/CD4+ cells combined with myosteatosis predict the prognosis in patients who underwent gastric cancer surgery. J Cachexia Sarcopenia Muscle 15: 1587-1600, 2024.
37. Shi W, Wang Y, Xu C, Li Y, Ge S, Bai B, Zhang K, Wang Y, Zheng N, Wang J, *et al*: Multilevel proteomic analyses reveal molecular diversity between diffuse-type and intestinal-type gastric cancer. Nat Commun 14: 835, 2023.
38. Khan M, Lin J, Wang B, Chen C, Huang Z, Tian Y, Yuan Y and Bu J: A novel necroptosis-related gene index for predicting prognosis and a cold tumor immune microenvironment in stomach adenocarcinoma. Front Immunol 13: 968165, 2022.
39. Zhao S, Wu Y, Wei Y, Xu X and Zheng J: Identification of biomarkers associated with CD8+ T cells in coronary artery disease and their pan-cancer analysis. Front Immunol 13: 876616, 2022.
40. Zhang F and Luo H: Diosmetin inhibits the growth and invasion of gastric cancer by interfering with M2 phenotype macrophage polarization. J Biochem Mol Toxicol 37: e23431, 2023.
41. Qu Y, Wang X, Bai S, Niu L, Zhao G, Yao Y, Li B and Li H: The effects of TNF-α/TNFR2 in regulatory T cells on the microenvironment and progression of gastric cancer. Int J Cancer 150: 1373-1391, 2022.
42. Jian F, Yanhong J, Limeng W, Guoping N, Yiqing T, Hao L and Zhaoji P: TIMP2 is associated with prognosis and immune infiltrates of gastric and colon cancer. Int Immunopharmacol 110: 109008, 2022.
43. Wei C, Chen M, Deng W, Bie L, Ma Y, Zhang C, Liu K, Shen W, Wang S, Yang C, *et al*: Characterization of gastric cancer stem-like molecular features, immune and pharmacogenomic landscapes. Brief Bioinform 23: bbab386, 2022. Wang P, Gu Y, Yang J, Qiu J, Xu Y, Xu Z, Gao J and Wan C: The prognostic value of NLRP1/NLRP3 and its relationship with immune infiltration in human gastric cancer. Aging (Albany NY) 14: 9980-10008, 2022.
44. Hamarsheh S and Zeiser R: NLRP3 inflammasome activation in cancer: A double-edged sword. Front Immunol 11: 1444, 2020.

45. Ohnishi N, Yuasa H, Tanaka S, Sawa H, Miura M, Matsui A, Higashi H, Musashi M, Iwabuchi K, Suzuki M, *et al*: Transgenic expression of *Helicobacter pylori* CagA induces gastrointestinal and hematopoietic neoplasms in mouse. Proc Natl Acad Sci USA 105: 1003-1008, 2008.
46. Marangoni F, Zhakyp A, Corsini M, Geels SN, Carrizosa E, Thelen M, Mani V, Prüßmann JN, Warner RD, Ozga AJ, *et al*: Expansion of tumor-associated Treg cells upon disruption of a CTLA-4-dependent feedback loop. Cell 184: 3998-4015.e19, 2021.
47. Zhang W, Zhang Q, Yang N, Shi Q, Su H, Lin T, He Z, Wang W, Guo H and Shen P: Crosstalk between IL-15Rα^{+} tumor-associated macrophages and breast cancer cells reduces CD8^{+} T cell recruitment. Cancer Commun (Lond) 42: 536-557, 2022.
48. Dixon KO, Tabaka M, Schramm MA, Xiao S, Tang R, Dionne D, Anderson AC, Rozenblatt-Rosen O, Regev A and Kuchroo VK: TIM-3 restrains anti-tumour immunity by regulating inflammasome activation. Nature 595: 101-106, 2021.
49. Lu F, Zhao Y, Pang Y, Ji M, Sun Y, Wang H, Zou J, Wang Y, Li G, Sun T, *et al*: NLRP3 inflammasome upregulates PD-L1 expression and contributes to immune suppression in lymphoma. Cancer Lett 497: 178-189, 2021.
50. Chen Y, Ye X, Escames G, Lei W, Zhang X, Li M, Jing T, Yao Y, Qiu Z, Wang Z, *et al*: The NLRP3 inflammasome: Contributions to inflammation-related diseases. Cell Mol Biol Lett 28: 51, 2023.